

Appendix for “ProxyFormer: Proxy Alignment Assisted Point Cloud Completion with Missing Part Sensitive Transformer”

Anonymous CVPR submission

Paper ID 10370

1. Overview

In this supplementary material, we provide additional information to complement the manuscript. First, we provide the details of missing part extractor in Sec. 2. Second, we present additional implementation details and experimental settings of *ProxyFormer* (Sec. 3). At last, we do more ablation studies and visualize more qualitative results of our method on the PCN dataset and ShapeNet-55/34. We also present detailed quantitative results on ShapeNet-55 and ShapeNet-34. (Sec. 4).

2. Missing Part Extractor

The given complete point cloud and incomplete point cloud of some point cloud completion common datasets such as PCN are not in the same scale of coordinate systems. So it is not possible to simply use the set difference operation to obtain the missing part. So we design a missing part extractor based on point-to-point and point-to-plane distances [4]. Fig. 1 is a detailed description of the missing part extractor.

Let \mathbf{A} and \mathbf{B} denote the Ground Truth (GT) and the incomplete point cloud, respectively. Firstly, we use the normal vector estimation method [5] to obtain the normal vector of each point in \mathbf{B} . For each point p_i , we assume the covariance matrix \mathcal{C} as follows:

$$\begin{aligned} \mathcal{C} &= \frac{1}{k} \sum_{i=1}^k (\mathbf{p}_i - \bar{\mathbf{p}}) \cdot (\mathbf{p}_i - \bar{\mathbf{p}})^T, \\ \mathcal{C} \cdot \vec{\mathbf{v}}_j &= \lambda_j \cdot \vec{\mathbf{v}}_j, j \in \{0, 1, 2\}. \end{aligned} \quad (1)$$

Here k refers to the k points closest to p_i . $\bar{\mathbf{p}}$ is the centroid of the nearest neighbor. λ_j is the j^{th} eigenvalue and $\vec{\mathbf{v}}_j$ is the j^{th} eigenvector. Then, the eigenvector corresponding to the largest eigenvalue is selected and normalized as the normal vector of the point.

After the calculation of the normal vector, the KNN algorithm is used to obtain the index of the corresponding adjacent points between the GT and the incomplete point cloud, which can be expressed as: $idx = KNN(\mathbf{A}, \mathbf{B}, K = 1)$.

According to this index, we go to \mathbf{B} to find the points b_i ($i \in idx$) and normal vectors n_i ($i \in idx$) of the adjacent points. Here we denote the point cloud composed of b_i as \mathbf{R} (it contains N points and the value of each point comes from the incomplete input, but they are one-to-one correspondence with points in GT), and denote the set of normal vectors n_i corresponding to each point in the point cloud \mathbf{R} as \mathbb{N} .

Then as shown in Fig. 2, we calculate the point-to-point distance and the point-to-plane distance as follows.

(1) For a point a_i in point cloud \mathbf{A} , i.e., the blue point in the figure, a corresponding point r_j in the point cloud \mathbf{R} can be found, i.e., the orange point in the figure. Vice versa.

(2) Similarly, we can get the corresponding normal vector n_j from \mathbb{N} .

(3) We connect point r_j to point a_i to calculate an error vector whose length is the point-to-point distance, i.e.,

$$D_{a_i, r_j}^{c2c} = \|E(i, j)\|_2. \quad (2)$$

(4) We project the error vector $E(i, j)$ along the direction of normal vector n_j to get another error vector $\hat{E}(i, j)$ whose length is the point-to-plane distance, i.e.,

$$D_{a_i, r_j}^{c2p} = \|\hat{E}(i, j)\|_2 = \frac{E(i, j) \cdot n_j}{\|n_j\|_2} = \|E(i, j) \cdot n_j\|_2. \quad (3)$$

(5) We use the weighted sum of the two distances as a comparison condition,

$$D = \alpha D_{a_i, r_j}^{c2c} + \beta D_{a_i, r_j}^{c2p}, \quad (4)$$

where $\alpha = 0.2$ and $\beta = 0.8$.

We perform the above operations on each point in the GT \mathbf{A} . If the calculated distance of the point is less than or equal to the preset threshold of 0.01, the point is stored in the set of existing parts, otherwise, it is stored in the set of missing parts. This process can be formulated as,

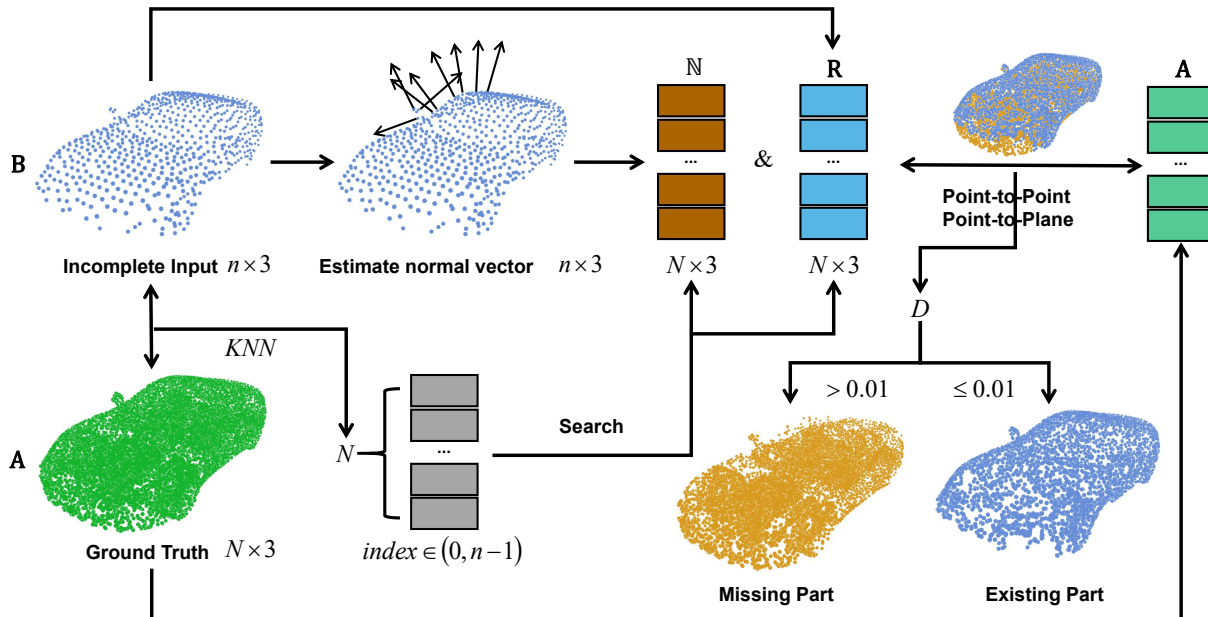


Figure 1. The pipeline of Missing Part Extractor. N is the count of points in ground truth and n is the count of points in incomplete input. Firstly, normal vectors are estimated for the incomplete input **B**. Secondly, the KNN algorithm is used to obtain the index with the shortest distance in **B** corresponding to each point in the ground truth **A**. A set of points **R** and a set of normal vectors **N** are obtained according to the index. Finally, we use **R**, **N** and **A** to calculate the point-to-point distance and the point-to-plane distance. The weighted sum D of these two distances is used for comparison with a pre-defined threshold 0.01. If the distance is less than or equal to the threshold, the point belongs to the existing part, otherwise it belongs to the missing part.

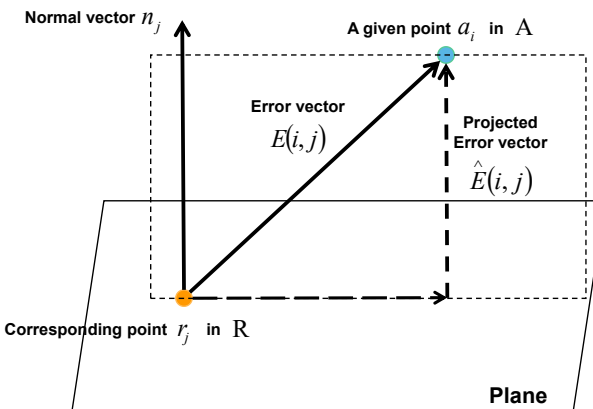


Figure 2. Point-to-point and point-to-plane distance. We use vector calculations to get the two distances. a_i is a point in point cloud **A** and r_j is the corresponding point in **R**. n_j is the normal vector of point r_j . The error vector $E(i, j)$ is computed by connecting point r_j to point a_i . The projected error vector $\hat{E}(i, j)$ is the new error vector after $E(i, j)$ is projected along the normal vector n_j .

$$a_i \in \begin{cases} \text{Existing part} & \text{if } D \leq 0.01 \\ \text{Missing part} & \text{else} \end{cases}, \forall a_i \in \mathbf{A}. \quad (5)$$

The missing part is separated from the GT by the above

method, and then downsampled to the same number as the incomplete input point for subsequent use. In Fig. 3, we show some results of missing part extractor.

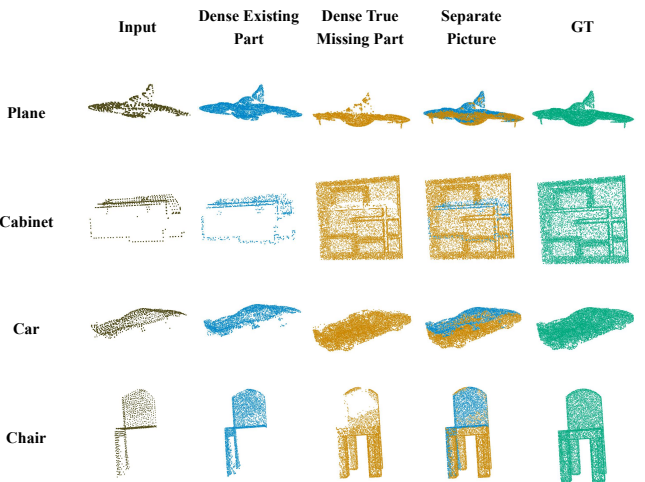


Figure 3. Some results of missing part extractor. From left to right are input, dense existing part, dense missing part, the splicing of the two and GT. From top to bottom are cases in four categories plane, cabinet, car and chair.

216	3. Implementation Details	270
217	In this section, we provide additional implementation de-	271
218	tails of the proposed <i>ProxyFormer</i> .	272
219		273
220		274
221	3.1. Basic experimental setup	275
222	We use Pytorch [2] for our implementation. All network	276
223	are trained on a single NVIDIA GeForce RTX 3090 graphi-	277
224	cs card. AdamW optimizer [1] is used to train the net-	278
225	work with initial learning rate as $5e - 4$ and weight decay	279
226	as $5e - 4$. When training on the PCN dataset, we set the	280
227	batch size to 64 and train the model for 400 epochs with the	281
228	continuous learning rate decay of 0.95 for every 20 epochs.	282
229	When training on ShapeNet-55/34, we set the batch size to	283
230	128 and train the model for 300 epochs with the continuous	284
231	learning rate decay of 0.83 for every 20 epochs.	285
232		286
233	3.2. Four types of proxies	287
234		288
235	There are four types of proxies during training, existing	289
236	proxies (<i>EP</i>), missing proxies (<i>MP</i>), true missing proxies	290
237	(<i>true-MP</i>), predicted missing proxies (<i>pre-MP</i>). <i>true-MP</i>	291
238	is not available during testing. When training on the PCN	292
239	dataset [9], <i>EP</i> is a 128×384 matrix and <i>MP</i> , <i>true-MP</i>	293
240	and <i>pre-MP</i> are both 224×384 matrices. When training on	294
241	the ShapeNet-55/34 [8], <i>EP</i> is a 128×384 matrix and <i>MP</i> ,	295
242	<i>true-MP</i> and <i>pre-MP</i> are both 96×384 matrices.	296
243		297
244	3.3. Feature and Position Extractor	298
245		299
246	Feature Extraction. We use farthest point sampling [3]	300
247	(FPS) to downsample the point cloud and use point trans-	301
248	former [10] (PT) to help exchange information between lo-	302
249	calized feature vectors. First we use an shared MLP to up-	303
250	scale the 3D coordinates of the point cloud to 32-dim as	304
251	features. Suppose the set of input point cloud is P_i , at each	305
252	downsampling stage: (1) perform farthest point sampling in	306
253	P_i and form a new set P_o ($P_o \subset P_i$); (2) a kNN graph is	307
254	performed on the P_i (we use $k = 16$ in our experiments);	308
255	(3) local max pooling is used to aggregate the features of	309
256	nearby k points to the current center point; (4) enhance fea-	310
257	tures with point transformer block.	311
258	On both PCN and ShapeNet-55/34 datasets, the number	312
259	of incomplete point cloud points input is $P = 2048$. De-	313
260	tailed network architecture is as follows:	314
261	incomplete input (2048×3) \rightarrow shared-MLP (2048×3	315
262	to 2048×32) \rightarrow FPS (2048×32 to 512×128) \rightarrow PT	316
263	(512×128 to 512×128) \rightarrow FPS (512×128 to 128×384)	317
264	\rightarrow PT (128×384 to 128×384).	318
265	On PCN (ShapeNet-55/34) dataset, the number of miss-	319
266	ing part points input is $P = 3584(\mathbf{1536})$. Bold numbers	320
267	correspond to the settings on ShapNet-55/34. The process	321
268	of FAPE is:	322
269	missing part ($3584(\mathbf{1536}) \times 3$) \rightarrow shared-MLP	323
	($3584(\mathbf{1536}) \times 3$ to $3584(\mathbf{1536}) \times 32$) \rightarrow FPS	
	($3584(\mathbf{1536}) \times 32$ to $896(\mathbf{384}) \times 128$) \rightarrow PT ($896(\mathbf{384}) \times 128$	
	to $896(\mathbf{384}) \times 128$) \rightarrow FPS ($896(\mathbf{384}) \times 128$ to $224(\mathbf{96}) \times 384$)	
	\rightarrow PT ($224(\mathbf{96}) \times 384$ to $224(\mathbf{96}) \times 384$).	
	Position Extraction. In order to keep the final position di-	
	mension consistent with the feature dimension extracted in	
	the previous step, we set both C_2 and C_{out} in the main text	
	to 384. Suppose the set of center points is P_c and the final	
	feature of feature extraction is F_c . Perform k -neighbor (we	
	use $k = 16$ in our experiments) subtraction (k NN-sub) and	
	aggregation (k NN-agg) operations on P_c and F_c , respec-	
	tively.	
	On both PCN and ShapeNet-55/34 datasets, the number	
	of incomplete center points input is $n = 128$. Detailed net-	
	work architecture is as follows:	
	P_c (128×3) \rightarrow k NN-sub (128×3 to $128 \times 16 \times 3$) \rightarrow	
	k NN-agg ($128 \times 16 \times 3$ to 128×3) ,	
	F_c (128×384) \rightarrow k NN-sub (128×384 to $128 \times 16 \times 384$)	
	\rightarrow k NN-agg ($128 \times 16 \times 384$ to 128×384) ,	
	$[P_c, F_c]$ (128×387) \rightarrow shared-MLP (128×387 to $128 \times$	
	384) .	
	On PCN (ShapeNet-55/34) dataset, the number of miss-	
	ing part center points input is $n = 224(\mathbf{96})$. Bold numbers	
	correspond to the settings on ShapNet-55/34. Detailed net-	
	work architecture is as follows:	
	P_c ($224(\mathbf{96}) \times 3$) \rightarrow k NN-sub ($224(\mathbf{96}) \times 3$ to $224(\mathbf{96}) \times$	
	16×3) \rightarrow k NN-agg ($224(\mathbf{96}) \times 16 \times 3$ to $224(\mathbf{96}) \times 3$) ,	
	F_c ($224(\mathbf{96}) \times 384$) \rightarrow k NN-sub ($224(\mathbf{96}) \times 384$ to	
	$224(\mathbf{96}) \times 16 \times 384$) \rightarrow k NN-agg ($224(\mathbf{96}) \times 16 \times 384$ to	
	$224(\mathbf{96}) \times 384$) ,	
	$[P_c, F_c]$ ($224(\mathbf{96}) \times 387$) \rightarrow shared-MLP ($224(\mathbf{96}) \times 387$	
	to 128×384) .	
	Subsequent attention score calculations do not affect the	
	dimension of this feature.	
	3.4. Missing Part Prediction	
	In the main text we have mentioned using the incom-	
	plete seed feature to generate coarse missing part. When	
	training on PCN dataset, the predicted coarse missing part	
	contains 224 points and the predicted dense missing part	
	contains 14336 points. When training on ShapeNet-55/34,	
	the predicted coarse missing part contains 96 points and the	
	predicted dense missing part contains 6144 points.	
	3.5. Missing Feature Generator	
	In Missing Feature Generator, we set N to 128 and M to	
	224 (on PCN dataset) or 96 (on ShapeNet-55/34). $C = 384$	
	and we divide the feature dimension equally into $U = 16$	
	groups.	
	3.6. Missing Part Sensitive Transformer	
	Like other transformer-based methods, we stack the miss-	
	ing part sensitive transformer and set its depth to 8.	

324
Multi-Head Self-Attention. This structural design al-
 325 lowes each attention mechanism to map to different spaces
 326 through Query, Key and Value to learn features. In this way,
 327 the different feature parts of each proxy are optimized, so as
 328 to make the proxies contain more diverse representations. In
 329 all our experiments, we set the number of multi-head atten-
 330 tion heads to 8.
 331 **Feed-Forward Network (FFN).** Referring to [6] and [8],
 332 we set up the feed-forward network as two linear layers with
 333 ReLU activation function and dropout.
 334

335 3.7. The calculation of DCD

336 Wu *et al.* [7] study the limitations of CD, believe that
 337 CD is not the optimal indicator for evaluating the visual
 338 quality of point cloud completion tasks, and proposed the
 339 density-aware chamfering distance (DCD), which can retain
 340 the measurement ability similar to CD and can also better
 341 judge the visual effect of the point cloud completion result.
 342 The formula for DCD is as follows:

$$343 d_{DCD}(S_1, S_2) = \frac{1}{2} \left(\frac{1}{|S_1|} \sum_{x \in S_1} \left(1 - \frac{1}{n_{\hat{y}}} e^{-\alpha \|x - \hat{y}\|_2} \right) \right) \\ 344 + \frac{1}{2} \left(\frac{1}{|S_2|} \sum_{y \in S_2} \left(1 - \frac{1}{n_{\hat{x}}} e^{-\alpha \|y - \hat{x}\|_2} \right) \right), \quad (6)$$

352 where $\hat{y} = \min_{y \in S_2} \|x - y\|_2$, $\hat{x} = \min_{y \in S_1} \|y - x\|_2$, and
 353 α denotes a temperature scalar, which we set to 1000, just
 354 as the original text describes.

355 4. Additional Ablation Studies and Experi- 356 mental Results

357 In this section, we first conduct more ablation experi-
 358 ments on some of the components used in *ProxyFormer*.
 359 Then, we present more qualitative and quantitative exper-
 360 imental results to further demonstrate the effectiveness of
 361 our method.

362 4.1. More ablation studies and analysis

363 **Feature Extractor.** We respectively replace the point trans-
 364 former with (1) a multilayer perceptron (MLP) composed of
 365 ordinary convolutional layers; (2) lightweight DGCNN; (3)
 366 traditional transformer using scalar attention. From Table
 367 1, we can know that the point transformer can better cap-
 368 ture the features of point clouds in the network structure
 369 proposed in this paper.

370 **Missing Feature Generator.** Many methods use the tiled
 371 copy of global feature as the feature of each point to gen-
 372 erate a complete point cloud. In this experiment, we make
 373 two attempts to the network after removing the missing fea-
 374 ture generator: (1) use random feature as the feature of *MP*;

Table 1. Ablation study on Feature Extractor of FAPE Module.

Method	CD-Avg
w/ MLP	8.08
w/ DGCNN	7.18
w/ Traditional Transformer (scalar attention)	7.53
w/ Point Transformer (vector attention)	6.77

(2) use the global feature (incomplete seed feature) as the
 373 feature of *MP*. From Table 2, we can see that the effect of
 374 using random feature and global feature is not ideal. Us-
 375 ing Missing Feature Generator, a more reasonable feature
 376 corresponding to the missing point can be generated from
 377 the feature of the existing points. Furthermore, experiments
 378 show that in the process of feature generation, evenly divid-
 379 ing the features into 16 groups can reduce the training time
 380 while reducing the CD of the final result to the lowest.

Table 2. Ablation study of Missing Feature Generator

Methods	Attempts	CD-Avg
w/o Missing Feature Generator	random feature	7.90
	copy global feature	8.49
w/ Missing Feature Generator	num of feature patch = 1	6.83
	num of feature patch = 8	6.80
	num of feature patch = 16	6.77
	num of feature patch = 32	6.85

Coarse missing part prediction. We try to use the pre-
 406 dicted missing seed feature to generate coarse missing part
 407 and did ablation experiments with this. The quantitative
 408 results on PCN dataset [9] are listed in Tables 3 and 4.
 409 Through this experiment, it can be proved that the features
 410 extracted from the partial input can better predict the ap-
 411 proximate position of the missing part (that is, the position
 412 of the center point of the coarse missing part). However, as
 413 analyzed in the main text, it is not enough to use only the
 414 features extracted from the partial input for the prediction
 415 of the missing details. Using Missing Feature Generator
 416 can better generates features that incorporate the missing
 417 details.

Model performance Analysis. In the main text, we have
 418 compared the complexity of our method with other meth-
 419 ods on the PCN dataset, and here we show the evaluation
 420 time of each method on ShapeNet-55/34 (all methods are
 421 tested on the same device, *i.e.* NVIDIA GeForce RTX 3090
 422 graphics card). The ShapeNet-55 dataset contains 10518
 423 test models. The ShapeNet-34 contains 3400 models in 34
 424 visible categories and 2305 models in 21 novel categories.
 425 Since 8 viewpoints are fixed for each model during the test-
 426 ing process, and the average of the results of the 8 view-
 427 points is used as the final CD value, the testing process is
 428 also time consuming. In Fig. 4, we show the comparison of
 429 *ProxyFormer* with other methods on ShapeNet-55/34 with
 430

432 Table 3. Ablation study on feature used for generating predicted coarse missing part. For CD, lower is better. 486
433 487

Methods	Chamfer Distance(10^{-3})								
	Air	Cab	Car	Cha	Lam	Sof	Tab	Ves	Ave
ProxyFormer(using predicted missing seed feature)	4.13	9.22	8.01	7.57	5.60	9.11	6.43	6.28	7.04
ProxyFormer(using incomplete seed feature)	4.01	9.01	7.88	7.11	5.35	8.77	6.03	5.98	6.77

439 Table 4. Ablation study on feature used for generating predicted coarse missing part. For DCD, lower is better. 493
440 494

Methods	Density-aware Chamfer Distance								
	Air	Cab	Car	Cha	Lam	Sof	Tab	Ves	Ave
ProxyFormer(using predicted missing seed feature)	0.572	0.604	0.611	0.597	0.609	0.641	0.530	0.579	0.593
ProxyFormer(using incomplete seed feature)	0.555	0.590	0.597	0.571	0.562	0.626	0.518	0.507	0.577

446 evaluation time (Eval. time) vs. CD, DCD and F1-Score. 500
447 For Eval. time vs. CD and DCD, the closer the value is to 501
the origin of the coordinates, the better the model 502 performance (that is, the smaller CD and DCD can be obtained 503 while the inference speed is fast). For Eval. time vs. 504 F1-Score, the closer the value is to the coordinates (0, 1), the 505 better the model performance (that is, the higher the F1- 506 Score can be obtained while the inference speed is fast). 507 From the pictures, we can observe that our proposed 508 *ProxyFormer* has the fastest inference speed while achieving 509 the smallest DCD and the highest F1-Score on ShapeNet-55/34. 510

4.2. More experimental results

511 **Three-views drawings.** In Figs. 5 and 6, we have drawn 512 three views of *ProxyFormer* on the PCN dataset, and we can 513 see that proxy alignment plays a significant role in the point 514 cloud completion task.

515 **More qualitative results on PCN dataset.** We show more 516 visualization results of *ProxyFormer* on PCN dataset in Fig. 517 7. From this, we can find that our method is more sensitive 518 to the concentrated distribution of missing part, which 519 makes it impossible to easily distinguish the shape of 520 objects from the existing point clouds, such as the second 521 cabinet and the first car. But our method can complete its 522 shape well, and the final result is basically consistent with GT.

523 **More qualitative results on ShapeNet-55/34.** In Figure 8, 524 we show the visualization results of point cloud completion 525 on ShapNet-55 by PoinTr [8], SeedFormer [11], and *ProxyFormer*. 526 We can intuitively see that *ProxyFormer* can better 527 complete the point cloud completion task. For example, 528 for the table in the first row, although the resulting shape 529 of PoinTr is complete, it fails to generate the details of the 530 bottom of the table well, and SeedFormer introduces some 531 noise points in the completion process, which affects the 532 final result. But our method is able to take both shape and 533 detail into account. Another example is the car in the fourth 534 row. The point cloud contains not only a car, but also a person. 535 There is a problem with the results of PoinTr and Seed- 536 Former completion, that is, the distribution of point clouds 537

538 is uneven, while *ProxyFormer* can better perceive the 539 distribution of missing points, thereby generating a more 540 reasonable complete point cloud. In Fig. 9, we also show more 541 visualization results of *ProxyFormer* on the ShapNet-55. To 542 better demonstrate the point cloud completion capability of 543 our method, for each object, we show two different parts 544 missing. For example, for the second bird house, we show 545 both cases where the bottom and top are missing, and our 546 method can easily get complete point clouds with local 547 details.

548 **Detailed quantitative results on ShapeNet-55/34.** We 549 report complete results of our method on ShapeNet-55 in 550 Tables 5 and 6 and results of novel categories on ShapeNet-34 551 in Tables 7 and 8. The models are tested under three 552 difficulty levels: simple, moderate and hard. We can see that 553 *ProxyFormer* achieves lowest DCD on almost all categories 554 on the three settings.

References

- [1] Ilya Loshchilov and Frank Hutter. Fixing weight decay regularization in adam. 2018. 3
- [2] Adam Paszke, Sam Gross, Francisco Massa, Adam Lerer, James Bradbury, Gregory Chanan, Trevor Killeen, Zeming Lin, Natalia Gimelshein, Luca Antiga, et al. Pytorch: An imperative style, high-performance deep learning library. *Advances in neural information processing systems*, 32, 2019. 3
- [3] Charles Ruizhongtai Qi, Li Yi, Hao Su, and Leonidas J Guibas. Pointnet++: Deep hierarchical feature learning on point sets in a metric space. *Advances in neural information processing systems*, 30, 2017. 3
- [4] Dong Tian, Hideaki Ochiaizu, Chen Feng, Robert Cohen, and Anthony Vetro. Geometric distortion metrics for point cloud compression. In *2017 IEEE International Conference on Image Processing (ICIP)*, pages 3460–3464. IEEE, 2017. 1
- [5] Federico Tombari, Samuele Salti, and Luigi Di Stefano. Unique signatures of histograms for local surface description. In *European conference on computer vision*, pages 356–369. Springer, 2010. 1

540

541

542

543

544

545

546

547

548

549

550

551

552

553

554

555

556

557

558

559

560

561

562

563

564

565

566

567

568

569

570

571

572

573

574

575

576

577

578

579

580

581

582

583

584

585

586

587

588

589

590

591

592

593

594

595

596

597

598

599

600

601

602

603

604

605

606

607

608

609

610

611

612

613

614

615

616

617

618

619

620

621

622

623

624

625

626

627

628

629

630

631

632

633

634

635

636

637

638

639

640

641

642

643

644

645

646

647

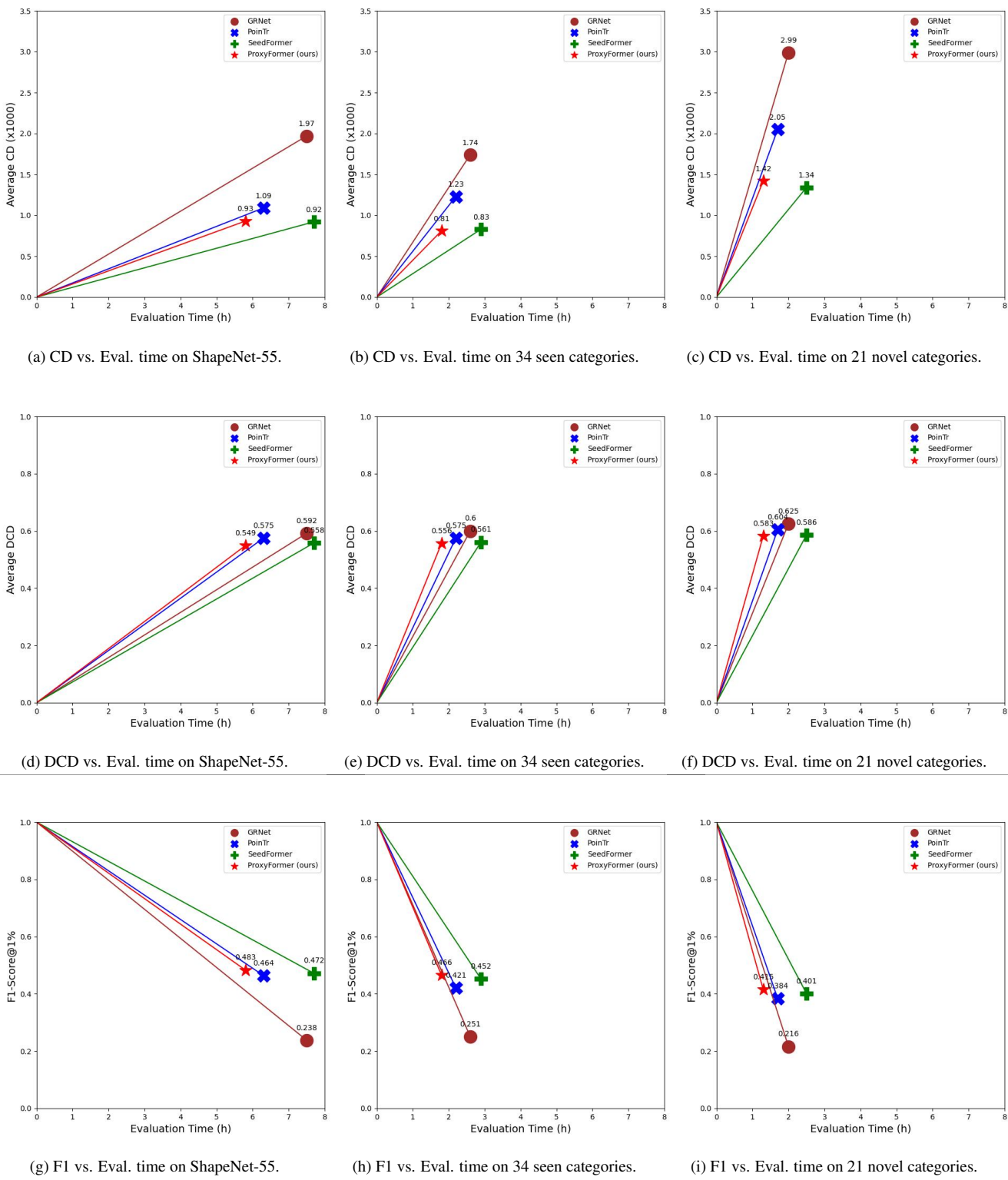
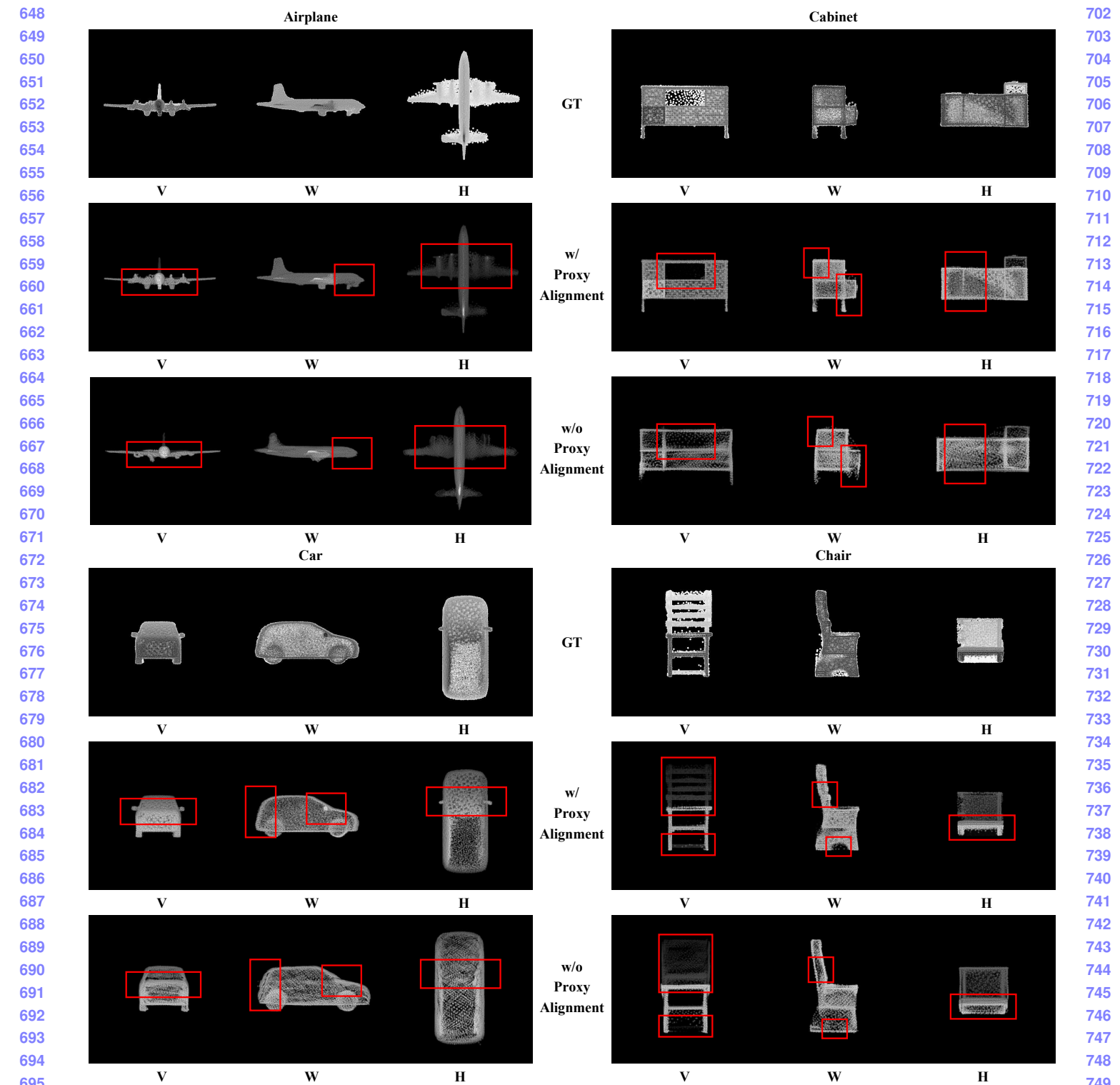
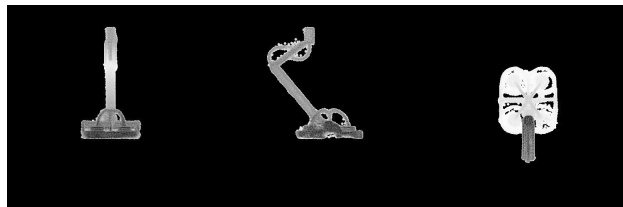


Figure 4. Performance comparison. The first column represents the comparison results on ShapeNet-55. The second column represents the comparison results on 34 seen categories in ShapeNet-34, and the third column represents the comparison results on 21 novel categories in ShapeNet-34. The first row represents Eval. time vs. CD. The second row represents Eval. time vs. DCD. The third row represents Eval. time vs. F1-Score@1%. In order to observe the distance between the values and the coordinates (0, 0) or (0, 1) more clearly, we connect them, so the lines in the figure have no practical meaning and are only used for comparison.



756
757
758
759
760
761
762
763

Lamp

764
765
766
767
768
769
770
771772
773
774
775
776
777
778

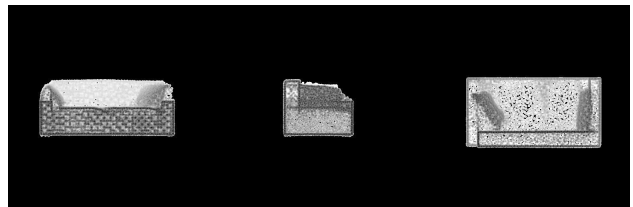
V

W

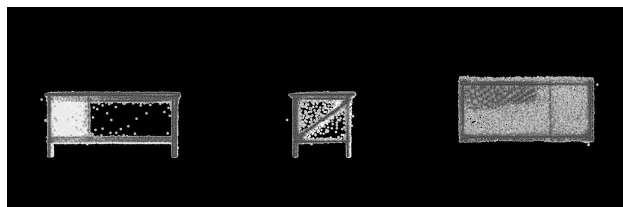
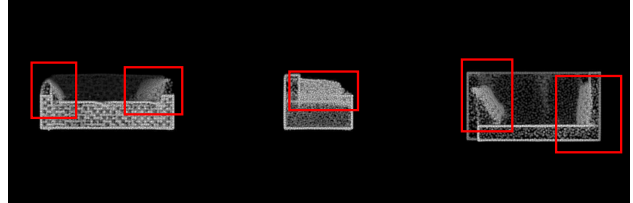
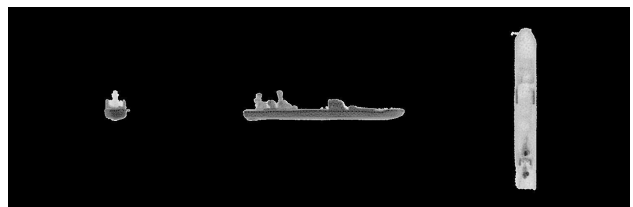
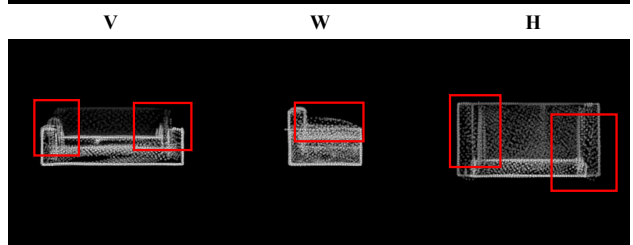
H

GT

Sofa

779
780
781
782
783
784
785
786
787
788
789
790
791
792
793
794
795
796
797
798
799
800
801
802

Table

803
804
805
806
807
808
809803
804
805
806
807
808
809w/
Proxy
Alignmentw/o
Proxy
Alignment

GT

Vessel

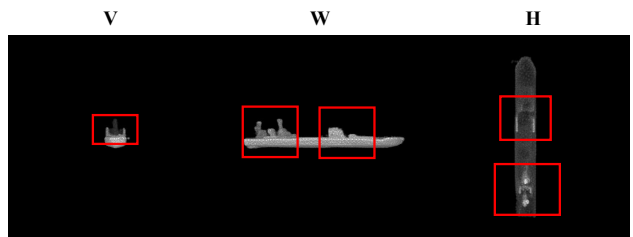
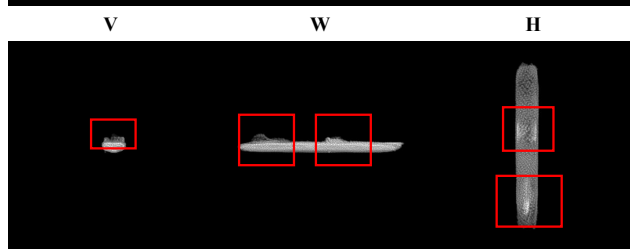
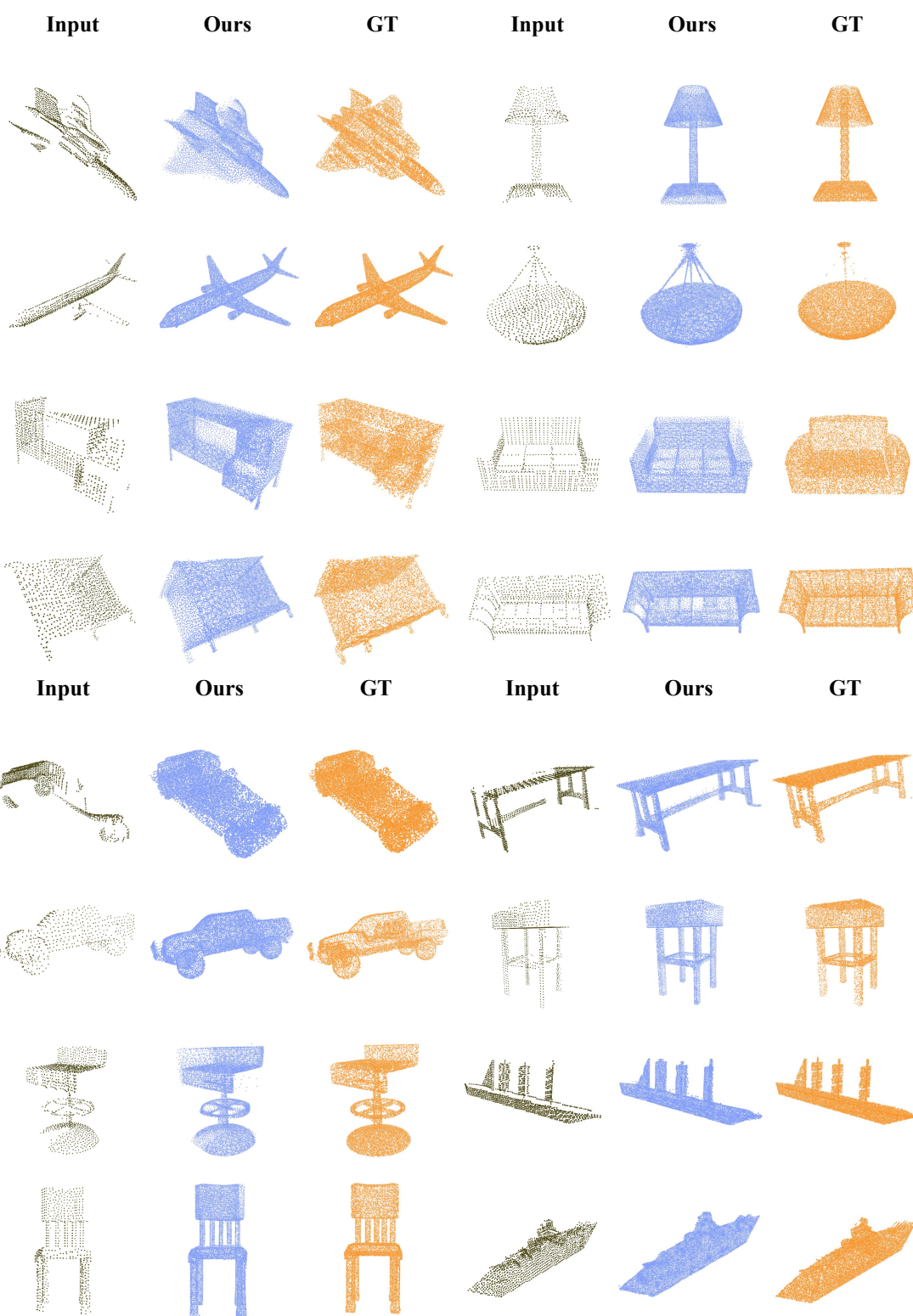
w/
Proxy
Alignmentw/o
Proxy
Alignment

Figure 6. Three-view drawings of GT, results with proxy alignment and results without proxy alignment. Each figure represents vertical plane (V), width plane (W) and horizontal plane (H) from left to right. The result six categories of objects in the PCN are listed separately, and the red box indicates where Proxy Alignment contributes the most.



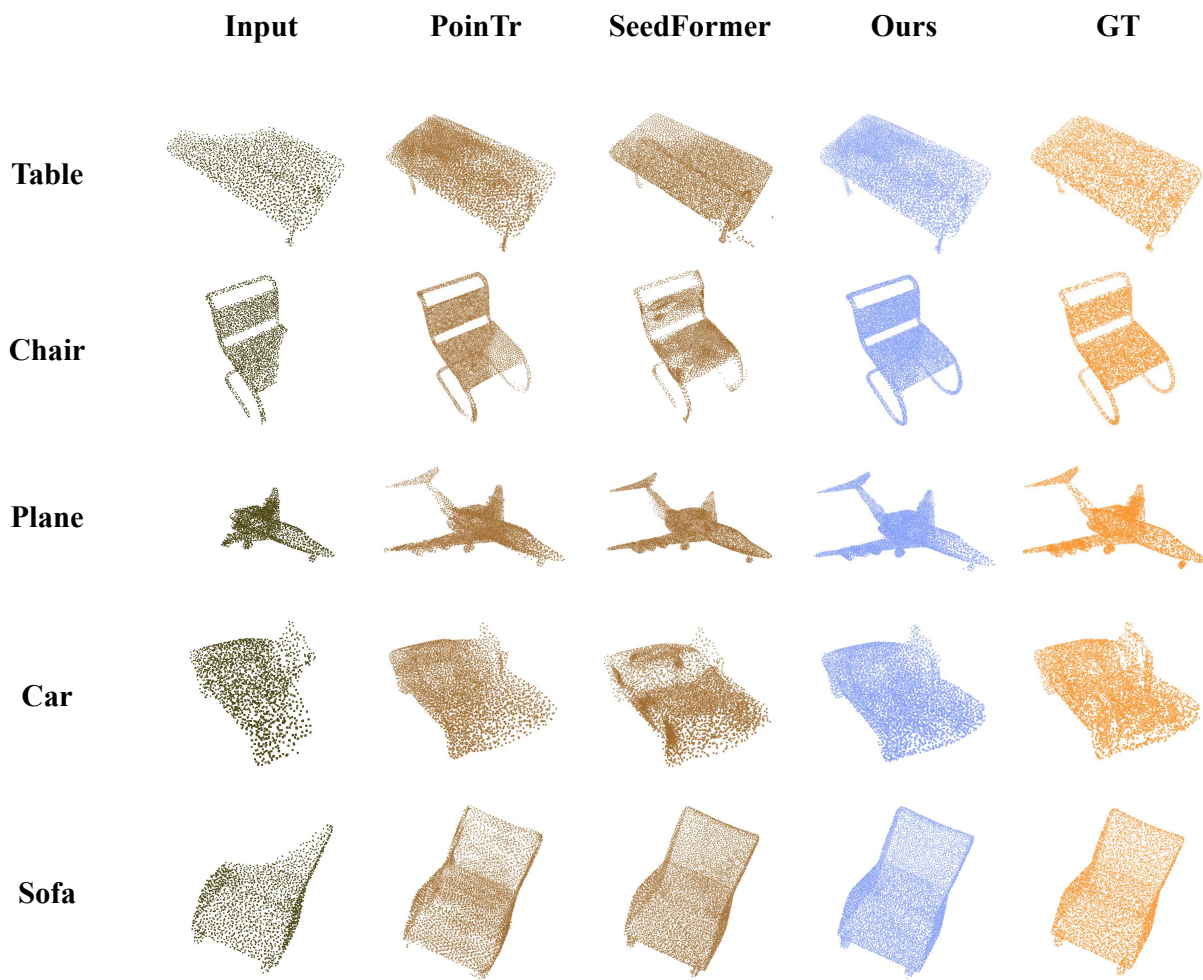
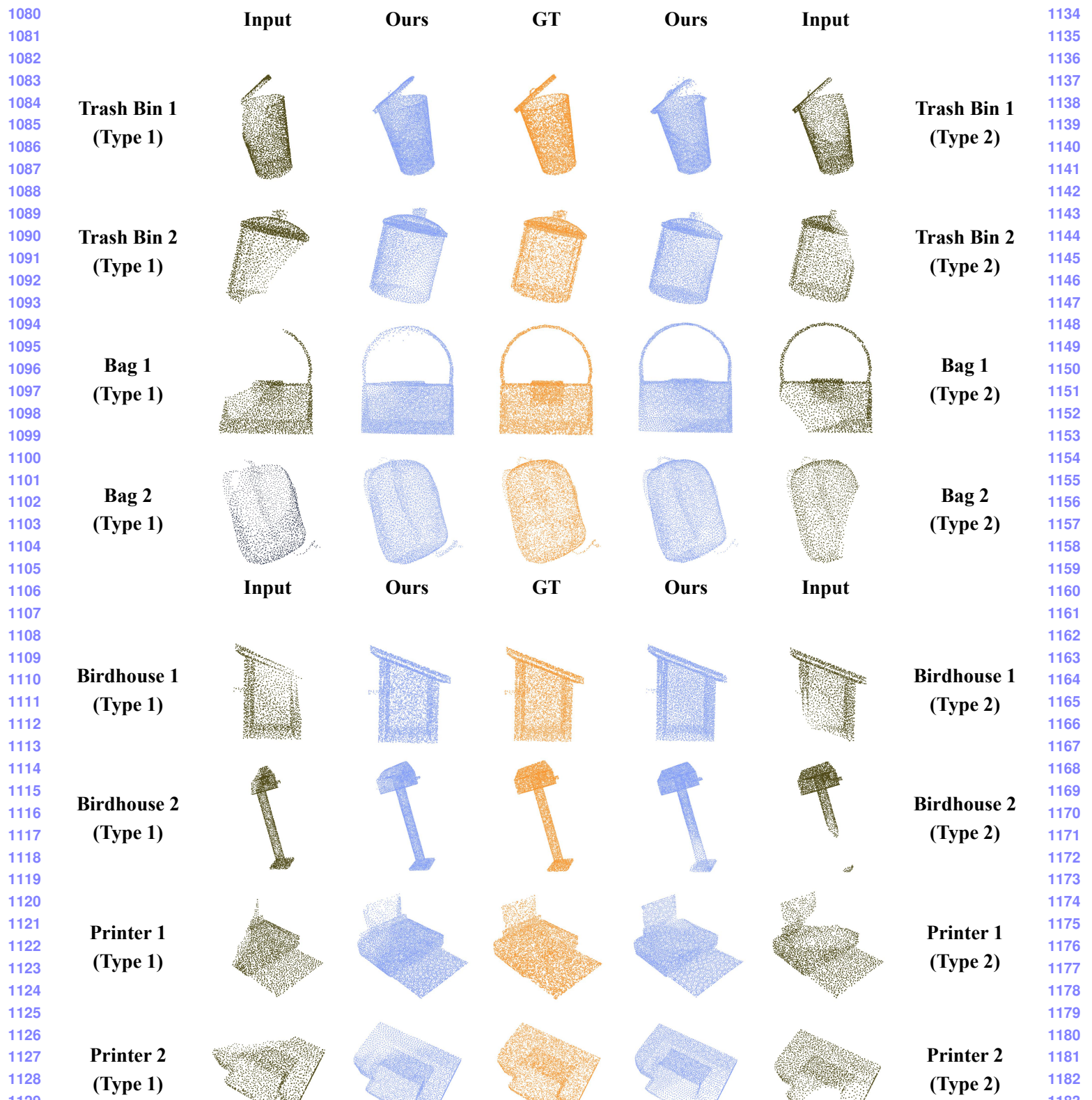


Figure 8. The visualization results of each method on ShapeNet-55, showing Table, Chair, Plane, Car and Sofa from top to bottom.

- 972
973
974
975
976
977
978
979
980
981
982
983
984
985
986
987
988
989
990
991
992
993
994
995
996
997
998
999
1000
1001
1002
1003
1004
1005
1006
1007
1008
1009
1010
1011
1012
1013
1014
1015
1016
1017
1018
1019
1020
1021
1022
1023
1024
1025
- [6] Ashish Vaswani, Noam Shazeer, Niki Parmar, Jakob Uszkoreit, Llion Jones, Aidan N Gomez, Łukasz Kaiser, and Illia Polosukhin. Attention is all you need. *Advances in neural information processing systems*, 30, 2017. 4
 - [7] Tong Wu, Liang Pan, Junzhe Zhang, Tai Wang, Ziwei Liu, and Dahua Lin. Density-aware chamfer distance as a comprehensive metric for point cloud completion. *arXiv preprint arXiv:2111.12702*, 2021. 4
 - [8] Xumin Yu, Yongming Rao, Ziyi Wang, Zuyan Liu, Jiwen Lu, and Jie Zhou. Pointr: Diverse point cloud completion with geometry-aware transformers. In *Proceedings of the IEEE/CVF international conference on computer vision*, pages 12498–12507, 2021. 3, 4, 5
 - [9] Wentao Yuan, Tejas Khot, David Held, Christoph Mertz, and Martial Hebert. Pcn: Point completion network. In *2018 International Conference on 3D Vision (3DV)*, pages 728–737. IEEE, 2018. 3, 4
 - [10] Hengshuang Zhao, Li Jiang, Jiaya Jia, Philip HS Torr, and Vladlen Koltun. Point transformer. In *Proceedings of the IEEE/CVF International Conference on Computer Vision*, pages 16259–16268, 2021. 3

- 1026
1027
1028
1029
1030
1031
1032
1033
1034
1035
1036
1037
1038
1039
1040
1041
1042
1043
1044
1045
1046
1047
1048
1049
1050
1051
1052
1053
1054
1055
1056
1057
1058
1059
1060
1061
1062
1063
1064
1065
1066
1067
1068
1069
1070
1071
1072
1073
1074
1075
1076
1077
1078
1079
- [11] Haoran Zhou, Yun Cao, Wenqing Chu, Junwei Zhu, Tong Lu, Ying Tai, and Chengjie Wang. Seedformer: Patch seeds based point cloud completion with upsample transformer. *arXiv preprint arXiv:2207.10315*, 2022. 5

Figure 9. More visual completion results of *ProxyFormer* on ShapeNet-55. Each object contains two missing angles.

1188 Table 5. Detailed results on the ShapeNet-55 dataset, including Simple (S), Moderate (M) and Hard (H) three difficulties. For CD- l_2
 1189 ($\times 1000$), lower is better. 1242
 1190 1243
 1191 1244
 1192 1245
 1193 1246
 1194 1247
 1195 1248
 1196 1249
 1197 1250
 1198 1251
 1199 1252
 1200 1253
 1201 1254
 1202 1255
 1203 1256
 1204 1257
 1205 1258
 1206 1259
 1207 1260
 1208 1261
 1209 1262
 1210 1263
 1211 1264
 1212 1265
 1213 1266
 1214 1267
 1215 1268
 1216 1269
 1217 1270
 1218 1271
 1219 1272
 1220 1273
 1221 1274
 1222 1275
 1223 1276
 1224 1277
 1225 1278
 1226 1279
 1227 1280
 1228 1281
 1229 1282
 1230 1283
 1231 1284
 1232 1285
 1233 1286
 1234 1287
 1235 1288
 1236 1289
 1237 1290
 1238 1291
 1239 1292
 1240 1293
 1241 1294
 1242 1295

		GRNet			PoinTr			SeedFormer			Ours		
		CD-S	CD-M	CD-H	CD-S	CD-M	CD-H	CD-S	CD-M	CD-H	CD-S	CD-M	CD-H
	airplane	0.87	0.87	1.27	0.27	0.38	0.69	0.23	0.35	0.61	0.21	0.28	0.54
	trash bin	1.69	2.01	3.48	0.80	1.15	2.15	0.73	1.08	1.94	0.70	1.04	1.98
	bag	1.41	1.70	2.97	0.53	0.74	1.51	0.43	0.67	1.28	0.39	0.65	1.34
	basket	1.65	1.84	3.15	0.73	0.88	1.82	0.65	0.83	1.54	0.64	0.74	1.40
	bathtub	1.46	1.73	2.73	0.64	0.94	1.68	0.52	0.82	1.45	0.52	0.85	1.47
	bed	1.64	2.03	3.70	0.76	1.10	2.26	0.63	0.91	1.89	0.62	0.91	2.04
	bench	1.03	1.09	1.71	0.38	0.52	0.94	0.32	0.42	0.84	0.30	0.39	0.80
	birdhouse	1.87	2.40	4.71	0.98	1.49	3.13	0.76	1.30	2.46	0.83	1.22	2.67
	bookshelf	1.42	1.71	2.78	0.71	1.06	1.93	0.57	0.84	1.57	0.55	0.92	1.73
	bottle	1.05	1.44	2.67	0.37	0.74	1.50	0.31	0.63	1.21	0.31	0.60	1.27
	bowl	1.60	1.77	2.99	0.68	0.78	1.44	0.56	0.65	1.18	0.54	0.62	1.14
	bus	1.06	1.16	1.48	0.42	0.55	0.79	0.42	0.55	0.73	0.40	0.46	0.59
	cabinet	1.27	1.41	2.09	0.55	0.66	1.16	0.57	0.69	1.05	0.64	0.59	1.00
	camera	2.14	3.15	6.09	1.10	2.03	4.34	0.83	1.68	3.45	0.82	1.77	4.04
	can	1.58	2.11	3.81	0.68	1.19	2.14	0.58	1.03	1.79	0.55	1.02	1.86
	cap	1.17	1.37	3.05	0.46	0.62	1.64	0.33	0.45	1.18	0.31	0.51	1.28
	car	1.29	1.48	2.14	0.64	0.86	1.25	0.65	0.86	1.17	0.61	0.69	1.03
	cellphone	0.82	0.91	1.18	0.32	0.39	0.60	0.31	0.40	0.54	0.26	0.38	0.45
	chair	1.24	1.56	2.73	0.49	0.74	1.63	0.41	0.65	1.38	0.40	0.61	1.48
	clock	1.46	1.66	2.67	0.62	0.84	1.65	0.53	0.74	1.35	0.50	0.67	1.45
	keyboard	0.74	0.81	1.09	0.30	0.39	0.45	0.28	0.36	0.45	0.27	0.33	0.43
	dishwasher	1.43	1.59	2.53	0.55	0.69	1.42	0.56	0.69	1.30	0.57	0.61	1.21
	display	1.13	1.38	2.29	0.48	0.67	1.33	0.39	0.59	1.10	0.46	0.62	1.18
	earphone	1.78	2.18	5.33	0.81	1.38	3.78	0.64	1.04	2.75	0.62	1.12	3.36
	faucet	1.81	2.32	4.91	0.71	1.42	3.49	0.55	1.15	2.63	0.49	1.16	3.01
	filecabinet	1.46	1.71	2.89	0.63	0.84	1.69	0.63	0.84	1.49	0.74	0.79	1.45
	guitar	0.44	0.48	0.76	0.14	0.21	0.42	0.13	0.19	0.32	0.14	0.20	0.28
	helmet	2.33	3.18	6.03	0.99	1.93	4.22	0.79	1.52	3.61	0.76	1.60	3.91
	jar	1.72	2.37	4.37	0.77	1.33	2.87	0.63	1.13	2.36	0.62	1.13	2.69
	knife	0.72	0.66	0.96	0.20	0.33	0.56	0.15	0.28	0.45	0.15	0.21	0.43
	lamp	1.68	2.43	5.17	0.64	1.40	3.58	0.45	1.06	2.67	0.42	1.05	3.03
	laptop	0.83	0.87	1.28	0.32	0.34	0.60	0.32	0.37	0.55	0.30	0.31	0.42
	loudspeaker	1.75	2.08	3.45	0.78	1.16	2.17	0.67	1.01	1.80	0.66	1.03	1.89
	mailbox	1.15	1.59	3.42	0.39	0.78	2.56	0.30	0.67	2.04	0.30	0.65	2.17
	microphone	2.09	2.76	5.70	0.70	1.66	4.48	0.62	1.61	3.66	0.59	1.58	3.98
	microwaves	1.51	1.72	2.76	0.67	0.83	1.82	0.63	0.79	1.47	0.61	0.69	1.35
	motorbike	1.38	1.52	2.26	0.75	1.10	1.92	0.68	0.96	1.44	0.67	0.96	1.49
	mug	1.75	2.16	3.79	0.91	1.17	2.35	0.79	1.03	2.06	0.75	0.92	2.00
	piano	1.53	1.82	3.21	0.76	1.06	2.23	0.62	0.87	1.79	0.55	0.85	1.73
	pillow	1.42	1.67	3.04	0.61	0.82	1.56	0.48	0.75	1.41	0.49	0.71	1.35
	pistol	1.11	1.06	1.76	0.43	0.66	1.30	0.37	0.56	0.96	0.34	0.52	0.90
	flowerpot	2.02	2.48	4.19	1.01	1.51	2.77	0.93	1.30	2.32	0.89	1.39	2.52
	printer	1.56	2.38	4.24	0.73	1.21	2.47	0.58	1.11	2.13	0.53	1.09	2.08
	remote	0.89	1.05	1.29	0.36	0.53	0.71	0.29	0.46	0.62	0.20	0.33	0.54
	rifle	0.83	0.77	1.16	0.30	0.45	0.79	0.27	0.41	0.66	0.21	0.32	0.50
	rocket	0.78	0.92	1.44	0.23	0.48	0.99	0.21	0.46	0.83	0.21	0.38	0.80
	skateboard	0.82	0.87	1.24	0.28	0.38	0.62	0.23	0.32	0.62	0.19	0.28	0.56
	sofa	1.35	1.45	2.32	0.56	0.67	1.14	0.50	0.62	1.02	0.49	0.57	1.01
	stove	1.46	1.72	3.22	0.63	0.92	1.73	0.59	0.87	1.49	0.68	0.88	1.67
	table	1.15	1.33	2.33	0.46	0.64	1.31	0.41	0.58	1.18	0.39	0.48	1.06
	telephone	0.81	0.89	1.18	0.31	0.38	0.59	0.31	0.39	0.55	0.28	0.32	0.48
	tower	1.26	1.69	3.06	0.55	0.90	1.95	0.47	0.84	1.65	0.46	0.82	1.67
	train	1.09	1.14	1.61	0.50	0.70	1.12	0.51	0.66	1.01	0.49	0.61	0.97
	watercraft	1.09	1.12	1.65	0.41	0.62	1.07	0.35	0.56	0.92	0.44	0.62	1.04
	washer	1.72	2.05	4.19	0.75	1.06	2.44	0.64	0.91	2.04	0.63	0.94	2.26
	mean	1.35	1.63	2.86	0.58	0.88	1.80	0.50	0.77	1.49	0.49	0.75	1.55

1296															1350
1297															1351
1298															1352
1299															1353
1300															1354
1301															1355
1302															1356
1303															1357
airplane	0.520	0.559	0.614	0.487	0.524	0.608	0.478	0.505	0.574	0.475	0.496	0.565			1358
trash bin	0.586	0.616	0.705	0.557	0.599	0.679	0.547	0.588	0.648	0.544	0.578	0.653			1359
bag	0.518	0.563	0.653	0.510	0.549	0.628	0.503	0.546	0.590	0.483	0.515	0.588			1360
basket	0.559	0.593	0.648	0.533	0.573	0.630	0.530	0.558	0.609	0.522	0.548	0.616			1361
bathhtub	0.503	0.553	0.646	0.499	0.544	0.619	0.498	0.523	0.609	0.492	0.519	0.589			1362
bed	0.553	0.620	0.694	0.544	0.589	0.661	0.537	0.583	0.637	0.528	0.554	0.622			1363
bench	0.528	0.546	0.607	0.507	0.531	0.589	0.506	0.504	0.543	0.483	0.494	0.539			1364
birdhouse	0.576	0.617	0.722	0.562	0.597	0.697	0.554	0.585	0.650	0.538	0.579	0.658			1365
bookshelf	0.563	0.589	0.678	0.541	0.569	0.655	0.523	0.562	0.623	0.519	0.554	0.631			1366
bottle	0.505	0.546	0.635	0.485	0.533	0.628	0.458	0.516	0.606	0.455	0.508	0.605			1367
bowl	0.545	0.591	0.676	0.531	0.560	0.641	0.524	0.529	0.613	0.507	0.529	0.602			1368
bus	0.533	0.559	0.606	0.525	0.547	0.599	0.521	0.525	0.584	0.499	0.523	0.570			1369
cabinet	0.590	0.593	0.643	0.557	0.577	0.626	0.532	0.548	0.595	0.521	0.544	0.596			1370
camera	0.583	0.647	0.728	0.558	0.615	0.701	0.547	0.608	0.670	0.535	0.584	0.671			1371
can	0.549	0.599	0.651	0.527	0.571	0.649	0.511	0.550	0.621	0.500	0.542	0.616			1372
cap	0.528	0.544	0.640	0.495	0.541	0.638	0.491	0.539	0.609	0.474	0.510	0.612			1373
car	0.614	0.660	0.683	0.581	0.631	0.673	0.566	0.607	0.661	0.565	0.592	0.644			1374
cellphone	0.508	0.509	0.568	0.483	0.506	0.541	0.482	0.497	0.520	0.458	0.480	0.521			1375
chair	0.526	0.559	0.623	0.505	0.555	0.620	0.501	0.527	0.609	0.488	0.523	0.606			1376
clock	0.543	0.578	0.657	0.528	0.561	0.634	0.515	0.554	0.594	0.502	0.531	0.595			1377
keyboard	0.515	0.528	0.553	0.499	0.511	0.541	0.477	0.498	0.510	0.473	0.483	0.515			1378
dishwasher	0.566	0.600	0.643	0.540	0.568	0.629	0.514	0.536	0.593	0.508	0.535	0.596			1379
display	0.532	0.544	0.595	0.517	0.544	0.587	0.483	0.519	0.554	0.483	0.508	0.560			1380
earphone	0.579	0.609	0.708	0.555	0.605	0.694	0.539	0.603	0.669	0.529	0.571	0.675			1381
faucet	0.512	0.602	0.681	0.502	0.573	0.687	0.495	0.565	0.663	0.483	0.548	0.665			1382
filecabinet	0.580	0.615	0.662	0.559	0.579	0.644	0.529	0.562	0.619	0.529	0.556	0.616			1383
guitar	0.499	0.538	0.616	0.488	0.514	0.602	0.459	0.495	0.571	0.456	0.493	0.578			1384
helmet	0.591	0.613	0.699	0.567	0.608	0.695	0.551	0.597	0.668	0.538	0.586	0.676			1385
jar	0.574	0.598	0.679	0.541	0.590	0.669	0.516	0.567	0.650	0.512	0.565	0.660			1386
knife	0.486	0.571	0.651	0.470	0.544	0.643	0.464	0.533	0.606	0.461	0.518	0.613			1387
lamp	0.526	0.587	0.717	0.520	0.581	0.689	0.510	0.578	0.677	0.488	0.553	0.657			1388
laptop	0.501	0.538	0.558	0.492	0.510	0.557	0.488	0.506	0.548	0.473	0.488	0.532			1389
loudspeaker	0.561	0.589	0.669	0.548	0.583	0.649	0.544	0.566	0.622	0.526	0.556	0.620			1390
mailbox	0.499	0.543	0.674	0.477	0.540	0.667	0.465	0.520	0.620	0.458	0.518	0.628			1391
microphone	0.546	0.622	0.709	0.511	0.587	0.701	0.503	0.579	0.681	0.490	0.560	0.674			1392
microwaves	0.559	0.580	0.634	0.546	0.566	0.621	0.541	0.544	0.614	0.522	0.544	0.597			1393
motorbike	0.653	0.690	0.714	0.623	0.657	0.709	0.614	0.652	0.687	0.596	0.627	0.695			1394
mug	0.582	0.618	0.706	0.560	0.588	0.678	0.536	0.585	0.657	0.535	0.569	0.644			1395
piano	0.550	0.585	0.658	0.538	0.573	0.632	0.537	0.552	0.611	0.519	0.544	0.602			1396
pillow	0.495	0.529	0.665	0.494	0.529	0.633	0.485	0.518	0.613	0.474	0.510	0.595			1397
pistol	0.557	0.586	0.668	0.529	0.571	0.655	0.509	0.570	0.620	0.506	0.545	0.627			1398
flowerpot	0.608	0.626	0.701	0.596	0.622	0.697	0.591	0.609	0.667	0.570	0.601	0.671			1399
printer	0.560	0.595	0.648	0.543	0.578	0.640	0.529	0.561	0.619	0.513	0.544	0.617			1400
remote	0.510	0.538	0.564	0.479	0.506	0.559	0.468	0.483	0.538	0.454	0.483	0.536			1401
rifle	0.534	0.572	0.626	0.519	0.562	0.646	0.500	0.551	0.632	0.497	0.539	0.616			1402
rocket	0.512	0.567	0.670	0.511	0.553	0.650	0.503	0.546	0.610	0.484	0.524	0.616			1403
skateboard	0.517	0.525	0.586	0.484	0.507	0.589	0.461	0.503	0.580	0.461	0.483	0.566			1404
sofa	0.554	0.588	0.603	0.532	0.559	0.596	0.525	0.541	0.563	0.507	0.523	0.567			1405
stove	0.562	0.577	0.650	0.528	0.554	0.634	0.521	0.550	0.601	0.516	0.546	0.606			1406
table	0.513	0.529	0.588	0.499	0.529	0.579	0.491	0.517	0.576	0.481	0.502	0.553			1407
telephone	0.506	0.532	0.564	0.483	0.498	0.554	0.467	0.495	0.529	0.457	0.476	0.516			1408
tower	0.571	0.622	0.676	0.536	0.593	0.684	0.513	0.567	0.659	0.512	0.562	0.649			1409
train	0.530	0.589	0.660	0.529	0.565	0.629	0.520	0.563	0.618	0.518	0.541	0.599			1410
watercraft	0.525	0.551	0.652	0.507	0.547	0.641	0.496	0.524	0.605	0.488	0.524	0.599			1411
washer	0.553	0.591	0.649	0.540	0.570	0.647	0.533	0.567	0.621	0.522	0.551	0.612			1412
mean	0.545	0.581	0.650	0.525	0.562	0.637	0.513	0.549	0.612	0.502	0.536	0.608			1413

1404

1405 Table 7. Detailed results on the 21 unseen categories of ShapeNet-34 dataset, including Simple (S), Moderate (M) and Hard (H) three
1406 difficulties. For CD- l_2 ($\times 1000$), lower is better.

1407

	GRNet			PoinTr			SeedFormer			Ours		
	CD-S	CD-M	CD-H	CD-S	CD-M	CD-H	CD-S	CD-M	CD-H	CD-S	CD-M	CD-H
bag	1.47	1.88	3.45	0.96	1.34	2.08	0.49	0.82	1.45	0.48	0.80	1.43
basket	1.78	1.94	4.18	1.04	1.40	2.90	0.60	0.85	1.98	0.57	0.91	2.08
birdhouse	1.89	2.34	5.16	1.22	1.79	3.45	0.72	1.19	2.31	0.51	1.03	2.00
bowl	1.77	1.97	3.90	1.05	1.32	2.40	0.60	0.77	1.50	0.63	0.96	1.79
camera	2.31	3.38	7.20	1.63	2.67	4.97	0.89	1.77	3.75	0.88	1.94	4.04
can	1.53	1.80	3.08	0.80	1.17	2.85	0.56	0.89	1.57	0.50	0.64	1.73
cap	3.29	4.87	13.02	1.40	2.74	8.35	0.50	1.34	5.19	0.51	1.57	6.38
keyboard	0.73	0.77	1.11	0.43	0.45	0.63	0.32	0.41	0.60	0.29	0.34	0.59
dishwasher	1.79	1.70	3.27	0.93	1.05	2.04	0.63	0.78	1.44	0.72	0.90	1.49
earphone	4.29	4.16	10.30	2.03	5.10	10.69	1.18	2.78	6.71	1.09	2.96	8.98
helmet	3.06	4.38	10.27	1.86	3.30	6.96	1.10	2.27	4.78	1.32	2.44	5.74
mailbox	1.52	1.90	4.33	1.03	1.47	3.34	0.56	0.99	2.06	0.74	1.09	2.14
microphone	2.29	3.23	8.41	1.25	2.27	5.47	0.80	1.61	4.21	0.73	1.73	3.70
microwaves	1.74	1.81	3.82	1.01	1.18	2.14	0.64	0.83	1.69	0.60	0.90	1.58
pillow	1.43	1.69	3.43	0.92	1.24	2.39	0.43	0.66	1.45	0.43	0.73	1.07
printer	1.82	2.41	5.09	1.18	1.76	3.10	0.69	1.25	2.33	0.59	1.40	2.56
remote	0.82	1.02	1.29	0.44	0.58	0.78	0.27	0.42	0.61	0.29	0.51	0.67
rocket	0.97	0.79	1.60	0.39	0.72	1.39	0.28	0.51	1.02	0.26	0.46	0.82
skateboard	0.93	1.07	1.83	0.52	0.80	1.31	0.35	0.56	0.92	0.35	0.61	0.78
tower	1.35	1.80	3.85	0.82	1.35	2.48	0.51	0.92	1.87	0.59	0.83	1.79
washer	1.83	1.97	5.28	1.04	1.39	2.73	0.61	0.87	1.94	0.62	0.89	1.90
mean	1.84	2.23	4.95	1.05	1.67	3.45	0.61	1.07	2.35	0.60	1.13	2.54

1432

1433

1434 Table 8. Detailed results on the 21 unseen categories of ShapeNet-34 dataset, including Simple (S), Moderate (M) and Hard (H) three
1435 difficulties. For DCD, lower is better.

1436

	GRNet			PoinTr			SeedFormer			Ours		
	DCD-S	DCD-M	DCD-H	DCD-S	DCD-M	DCD-H	DCD-S	DCD-M	DCD-H	DCD-S	DCD-M	DCD-H
bag	0.521	0.597	0.617	0.506	0.573	0.593	0.489	0.556	0.572	0.492	0.556	0.573
basket	0.599	0.631	0.633	0.574	0.621	0.626	0.555	0.605	0.613	0.548	0.608	0.614
birdhouse	0.610	0.678	0.708	0.580	0.658	0.680	0.561	0.632	0.659	0.554	0.615	0.641
bowl	0.603	0.637	0.659	0.581	0.624	0.631	0.558	0.595	0.614	0.553	0.597	0.616
camera	0.624	0.640	0.708	0.594	0.629	0.689	0.574	0.618	0.666	0.587	0.619	0.665
can	0.570	0.628	0.637	0.550	0.617	0.582	0.525	0.587	0.568	0.518	0.571	0.569
cap	0.632	0.737	0.783	0.598	0.715	0.757	0.568	0.689	0.743	0.560	0.692	0.742
keyboard	0.484	0.513	0.535	0.461	0.501	0.519	0.450	0.484	0.505	0.446	0.477	0.493
dishwasher	0.597	0.631	0.701	0.564	0.609	0.681	0.554	0.590	0.658	0.566	0.591	0.656
earphone	0.695	0.687	0.803	0.666	0.671	0.773	0.655	0.645	0.739	0.660	0.648	0.751
helmet	0.669	0.730	0.781	0.639	0.717	0.761	0.627	0.706	0.738	0.632	0.699	0.738
mailbox	0.563	0.571	0.627	0.547	0.552	0.605	0.526	0.536	0.582	0.518	0.541	0.581
microphone	0.618	0.717	0.764	0.585	0.700	0.746	0.573	0.672	0.732	0.566	0.734	
microwaves	0.609	0.622	0.660	0.575	0.604	0.634	0.557	0.582	0.623	0.549	0.584	0.622
pillow	0.595	0.620	0.626	0.575	0.606	0.603	0.562	0.577	0.578	0.556	0.578	0.568
printer	0.631	0.675	0.725	0.607	0.665	0.700	0.593	0.650	0.687	0.588	0.651	0.683
remote	0.496	0.516	0.542	0.480	0.494	0.526	0.462	0.480	0.508	0.456	0.470	0.507
rocket	0.499	0.510	0.560	0.476	0.501	0.542	0.457	0.488	0.518	0.449	0.469	0.516
skateboard	0.493	0.539	0.607	0.474	0.527	0.580	0.463	0.511	0.567	0.456	0.514	0.566
tower	0.545	0.602	0.685	0.526	0.590	0.667	0.500	0.563	0.655	0.494	0.544	0.656
washer	0.586	0.612	0.717	0.562	0.591	0.698	0.551	0.566	0.686	0.544	0.569	0.686
mean	0.583	0.623	0.670	0.558	0.608	0.647	0.541	0.587	0.629	0.538	0.584	0.627

1511